Contribution from the Lehrstuhl für Theoretische Chemie, Technische Universität München, 8 München 2, West Germany, and the Department of Chemistry, Queen's University, Kingston, Ontario K7L 3N6, Canada

SCF–Xα Scattered-Wave Studies on Bonding and Ionization Potentials. 2. Higher Valence State Sulfur Compounds

NOTKER RÖSCH,[1a] VEDENE H. SMITH, Jr.,*[1] and M. H. WHANGBO[1b]

Received March 10, 1976 AIC60191O

The nature of the bonding in hypervalent molecules is examined for the series SX_6 (X = F, Cl, H) as well as for SF_4 and SOF_4 by means of SCF–Xα scattered-wave calculations. We refine our method of "atoms-in-molecule" population analysis to distinguish different partial wave contributions in the individual atomic regions. For the SX_6 series, we discuss the correlation of electronegativity of the ligands (bond polarity) and the existence of these compounds. The bonding in SF_6 is affected in a different way by the ligand s orbitals than in SCl_6, a factor not included in the original theory of hypervalency. A detailed analysis of the nature of the bonding in SF_6 is made by using both the partial wave population analysis and orbital contour maps. A great similarity between the electronic structure of SF_4, SOF_4, and SF_6 is found which does not justify the usual distinction between hypervalent I (SF_4) and hypervalent II (SOF_4, SF_6) bonding. We find in agreement with experiment that the axial fluorine ligands in SF_4 have smaller F 1s ionization energies than the equatorial ligands. The first ionization potential of SOF_4 is smaller than that of SF_4 (14.5 vs. 16.2 eV).

The elements of groups 5–8 have the ability to form additional bonds beyond the number allowed by the Lewis–Langmuir valence theory when they are associated with electronegative atoms (primarily fluorines). For molecules which contain an element with its valency so expanded, Musher coined the descriptive name *hypervalent molecules*.[2]

There have been quite a number of suggestions to understand qualitatively the bonding of these molecules.[2-9] According to the perfect pairing model of Pauling[4] one has to invoke d-orbital participation on the central atom in constructing the appropriate orthogonal hybrid orbitals. In order to avoid the expense of a high promotional energy Dogett[5] introduced a simple valence-bond model without d-orbital participation by considering various valence-bond structures with charge transfer from the central atom to the ligands. This model leads to a formal charge on the central atom consistent with the fact that hypervalent molecules are mainly formed with electronegative ligands. The relation between the formal charge and the nature of the d orbitals on the central atom and thus the feasibility of the d-orbital participation in bonding have been studied by Coulson and Gianturco.[6,7]

Musher,[2a] on the other hand, gave a qualitative description of the bonding by simply using nonorthogonal hybrid orbitals on the central atom which also removes the necessity of d-orbital participation. He also discussed the molecular orbital (MO) equivalent of the theory together with CNDO/2 calculations of the simplest sulfur hydrides and fluorides.[2c,d] In the MO language hypervalent bonds may be characterized as three-center electron-rich bonds[8] with the further qualitative distinction of whether only atomic p orbitals are involved (type I) or whether sp mixing plays a significant role (type II). Chen and Hoffmann recently gave a molecular orbital analysis of the bonding in sulfuranes based on extended Hückel calculations.[9]

We have already reported SCF–Xα scattered-wave studies on SF_6, SeF_6, and TeF_6, which will be referred to as part 1.[10] In order to gain more insight into the bonding character of type II hypervalent sulfur compounds we have carried out SCF–Xα–SW calculations on SH_6 and SCl_6 which shall be compared to our previous results in part 1 for SF_6. We have further studied the electronic structure of some hypervalent sulfur compounds of low symmetry, namely, SF_4 and SOF_4. A comparison among these two and SF_6 should shed some light on Musher's distinction between type I and type II hypervalent molecules.

The purpose of this paper is not only to study the structure of hypervalent molecules but to continue along the lines of part 1 and to show how detailed knowledge about the molecular orbitals of a molecule, as furnished from an SCF–Xα–SW calculation, may be usefully reduced and correlated with the known chemistry of the molecule under study. Orbital contour maps displaying detailed features of the charge distribution in space, as well as a scheme similar to a conventional population analysis but suitably adapted to the form of SW orbitals, will be employed. To assess the reliability of these tools we will compare our findings to previous calculations of related compounds.[2,11] In particular a recent extensive Hartree–Fock study of the molecules SH_2, SH_4, and SH_6 which also included geometry optimization[11] will be used in this context.

Scattered-Wave Population Analysis

The SCF–Xα–SW method which we are using here has been shown to give reliable information on the electronic structure of a wide range of different molecules and clusters.[11] The essential features of the method are its use of the local exchange approximation, the muffin tin model for the electronic potential, and the scattered-wave (or multiple scattering) formalism to solve the one-particle Schrödinger equation. Because details of this method are well documented,[12] we shall not repeat them here. Two features of the SCF–Xα–SW method should be stressed, however, as they are of special importance in connection with the following investigations. The molecular orbital wave functions are represented as rapidly converging multicenter partial wave expansions whose radial parts are found through numerical integration. Thus all of the problems of an LCAO–MO method connected with the choice of proper basis functions may be avoided. A further consequence of this multicenter expansion of the orbital wave function is a *distribution of electronic charge over different regions of space*, as defined by the muffin tin model. The SCF–Xα–SW calculation starts with superimposed atomic distributions over the various regions of the molecule and reaches self-consistency at which point the molecular charge distribution is obtained. Thus the molecular charge distribution of each region[12d]—atomic (I), interatomic (II), and extramolecular (III)—and the change occurring during convergence to self-consistency provide information about the charge redistribution during formation of the bonds (see Figure 1 of part 1 for an illustration of the partitioning of space).

By analogy to the conventional Mulliken population analysis, we defined in part 1 the Xα–SW populations as in eq 1 and 2, where Q_I is the integrated electronic charge in the corresponding region of space and n_A and n_L are the total number of atomic spheres and the number of ligand spheres, respectively. Here, Z_I is the atomic number of atom I. In the

---

* To whom correspondence should be addressed at Queen's University.

$$\text{X}\alpha\text{–SW net atomic population} \equiv Q_{\text{I}} \tag{1a}$$

$$\text{X}\alpha\text{–SW net atomic charge} \equiv Z_{\text{I}} - Q_{\text{I}} \tag{1b}$$

$$\text{X}\alpha\text{–SW gross atomic population} \equiv Q_{\text{I}} + Q_{\text{II}}/n_{\text{A}} + Q_{\text{III}}/n_{\text{L}} \tag{2a}$$

$$\text{X}\alpha\text{–SW gross atomic charge} \equiv Z_{\text{I}} - (Q_{\text{I}} + Q_{\text{II}}/n_{\text{A}} + Q_{\text{III}}/n_{\text{L}}) \tag{2b}$$

case where this is the central atom the last term in eq 2 is not included in the Xα–SW gross atomic charge. When the distinction between the central atom and the ligands is not appropriate, e.g., in a diatomic molecule, one may define

$$\text{X}\alpha\text{–SW gross atomic charge} \equiv Z_{\text{I}} - Q_{\text{I}} - (Q_{\text{II}} + Q_{\text{III}})/n_{\text{A}} \tag{3}$$

For a number of questions it is helpful to have not only total atomic populations as given by eq 1 but also more detailed information concerning the relative contributions of the different atomic orbitals involved. Questions of such a nature include the amount of d-orbital participation in a molecule where their contribution to the various molecular orbitals is not singled out by the high symmetry as in octahedral molecules or the relative contribution of ligand s and p orbitals to the various σ bonds. Since the Xα–SW method[12d] uses in region I a partial wave expansion of the form

$$\Psi_{\text{I}}^{(\text{i})}(\mathbf{r}) = \sum_{lm} C_{lm}{}^{\text{i}} R_l{}^{\text{i}}(r_{\text{i}}) Y_{lm}(\mathbf{r}_{\text{i}}) \tag{4}$$

where the index i refers to a specific atom i, an obvious measure for the contribution of a specific atomic orbital to the molecular orbital under consideration is given by[13]

$$Q_{lm}{}^{(\text{i})} = 4\pi |C_{lm}{}^{\text{i}}|^2 \int_0^{b_{\text{i}}} [R_l{}^{\text{i}}(r_{\text{i}})]^2 r_{\text{i}}{}^2 \, \mathrm{d}r_{\text{i}} \tag{5}$$

b_{i} denotes the radius of the corresponding atomic sphere. Of course, one has

$$Q_{\text{I}} \equiv Q^{(\text{i})} = \sum_{lm} Q_{lm}{}^{(\text{i})} \tag{6a}$$

and

$$1 = \sum_{i} Q^{(\text{i})} + Q_{\text{II}} + Q_{\text{III}} \tag{6b}$$

If one compares the population analysis for Xα–SW molecular orbitals as outlined above to a conventional LCAO-type population analysis, one finds as a major difference that the latter relies on the overlap concept, whereas the former is based on an atoms-in-molecule point of view. This does not involve any bias toward a specific picture of the nature of the bonds but reflects the fundamental differences in the underlying mathematical formalisms that are used to solve the Schrödinger equation. Both methods of population analysis suffer from specific disadvantages limiting their practical value. In an LCAO-type analysis one has to arbitrarily divide the overlap density and very frequently has to face negative populations for certain orbitals (see, e.g., ref 11). While the SW approach avoids the basis set dependence found in an LCAO-type analysis, it does have some arbitrariness in the use of the atomic spheres and the assignment of the charge situated in the interatomic and the extramolecular regions. The sphere sizes occurring in the muffin tin potential are to a certain extent arbitrary parameters of the model and may only be loosely tied to the values of the corresponding covalent radii and/or determined by requiring minimal potential steps across the various boundaries of muffin tin regions. In order to eliminate the influence of the sphere sizes on our results we rely in our charge analysis more on changes between superposed atomic charges and the self-consistent molecular charge distribution or on changes in a series of related molecules. This limitation again finds its counterpart in the current practice of LCAO-type population analysis.

Results and Discussion

SX_6 Compounds. In part 1 we observed that a large amount of the electronic charge is drained away from the central atom to the fluorine ligands for the series of molecules SF_6, SeF_6, and TeF_6. In an attempt to assess the importance of the electronegativity of the ligands in making hypervalent molecules of the type ML_6, we varied the ligand atoms and performed SCF–Xα–SW calculations for SH_6 and SCl_6.

The molecules were assumed to have octahedral symmetry, of course. The bond lengths were taken from experiment (SF_6) and from a previous calculation[11] with geometry optimization (SH_6) or were determined approximately by scaling the bond length found experimentally in SCl_2 in the ratio of the corresponding bond length in SF_2 and SF_6 (for SCl_6): $d_{\text{S–H}}$ = 2.761 au, $d_{\text{S–Cl}}$ = 3.720 au, and $d_{\text{S–F}}$ = 2.956 au. The atomic sphere radii in the muffin tin potentials were determined for SF_6 (cf. part 1) by requiring touching spheres and a continuous potential at the points where they are in contact.[14] For SH_6, an additional calculation with the bond length $d_{\text{S–H}}$ = 2.5 au was performed, and in order to facilitate comparison between these two calculations for SH_6 and that for SF_6, the same sulfur sphere radius was chosen in all three cases. We will report only the first one, as they both lead to the same conclusions for the questions to be discussed below. For SCl_6 the sulfur sphere radius had to be enlarged in comparison with these molecules in order to account for the increased bond length and the changed ratio of the covalent radii (1:1). The resulting sphere radii for the sulfur sphere were 1.78, 1.86, and 1.78 au for SH_6, SCl_6, and SF_6, respectively. The ligand sphere radii are then completely determined: 0.981, 1.860, and 1.176 au for H, Cl, and F, respectively.

The values used for the atomic exchange constant α were taken as determined by Schwarz (α_{HF}),[15a] except for H.[15b] In the other regions a weighted average of these values has been used. Partial waves up through $l = 2$ were taken into account in the sulfur sphere, and through $l = 1$ in the ligand spheres. The iterations toward self-consistency were continued until the relative change in the potential was less than 10^{-2} at any point in space.

The calculated orbital energies for the valence electrons of the molecules SF_6 and SCl_6 are compared in Table I together with the normalized orbital charge distribution over the various regions of space. For SH_6 we find the following orbital energies: −1.621 Ry ($1a_{1g}$), −0.964 Ry ($1t_{1u}$), and −0.484 Ry ($1e_g$). No direct comparison with Hartree–Fock type orbital energies[2c,11] is possible because of the different concept of orbital energies in both the Hartree–Fock and Xα theory.[16] However, the general features in the orbital energy spectrum are the same (for SF_6 see part 1). In Figure 1 we compare the energies of all occupied valence orbitals together with those of the lowest unoccupied orbitals for SH_6, SCl_6, and SF_6.

Table I and Figure 1 reveal a fair similarity between the energy level spectra and spatial charge distributions of SF_6 and SCl_6. The energy levels of SCl_6 are shifted upward compared with those of SF_6. This is due to the fact that the chlorine s and p valence levels lie energetically much higher than those of fluorine and has important consequences for the electronic structure of SCl_6. The very low-lying $1a_{1g}$, $1t_{1u}$, and $1e_g$ valence levels, mainly attributed to ligand s orbitals, are not included in the qualitative discussions of the bonding of hypervalent molecules[2] yet do contribute to sulfur–ligand bonding as may also be confirmed by detailed orbital contour maps. The $1a_{1g}$ level plays a prominent role due to its large localization within the sulfur sphere (0.213 and 0.455 for SF_6 and SCl_6). The sulfur 3s atomic orbital contributes significantly to bond formation through the interaction with the ligand p orbitals in order to form hypervalent molecules of type

Table I. SCF–Xα–SW Orbital Energies and Normalized Charge Distributions in the Various Molecular Regions for the Valence Orbitals of SF_6 and SCl_6

	SF_6					SCl_6				
Orbital	$-\epsilon_i$[a]	S	F	INT	EXT	$-\epsilon_i$[a]	S	Cl	INT	EXT
$1a_{1g}$	2.633	0.213	0.083	0.271	0.015	2.111	0.455	0.050	0.244	0.002
$1t_{1u}$	2.413	0.062	0.112	0.242	0.025	1.749	0.083	0.113	0.225	0.015
$1e_g$	2.337	0.026	0.122	0.209	0.032	1.652	0.014	0.131	0.172	0.025
$2a_{1g}$	1.665	0.361	0.072	0.161	0.057	1.484	0.231	0.093	0.172	0.040
$2t_{1u}$	1.310	0.232	0.079	0.244	0.048	1.123	0.299	0.070	0.239	0.041
$1t_{2g}$	1.123	0.031	0.094	0.365	0.041	0.913	0.018	0.088	0.415	0.036
$2e_g$	1.006	0.091	0.112	0.166	0.070	0.747	0.081	0.110	0.184	0.075
$1t_{2u}$	0.962	0.0	0.113	0.289	0.032	0.760	0.0	0.106	0.331	0.035
$3t_{1u}$	0.961	0.018	0.110	0.281	0.042	0.772	0.032	0.097	0.343	0.042
$1t_{1g}$	0.889	0.0	0.122	0.236	0.033	0.669	0.0	0.117	0.257	0.039
$3a_{1g}$[b]	0.324	0.279	0.095	0.088	0.066	0.478	0.161	0.092	0.202	0.087
$4t_{1u}$						0.218	0.352	0.066	0.187	0.063

[a] Energies in rydberg units (1 Ry = 13.6 eV). [b] Orbitals listed below the dashed line (here and in other tables) are unoccupied in the ground state of the molecule.

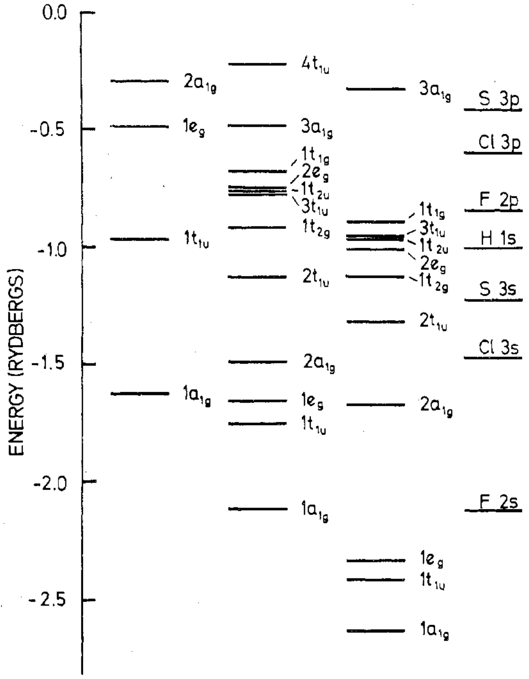

Figure 1. Comparison of the SCF–Xα–SW orbital energies for different molecules of type SX_6. The HOMO is the $1e_g$ orbital in SH_6 and the $1t_{1g}$ orbital in SCl_6 and SF_6. The SCF–Xα orbital energies for the various free atoms are also shown.

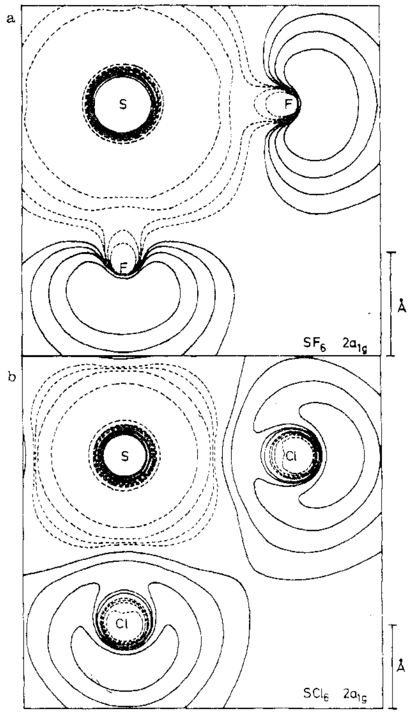

Figure 2. Contour plots of the $2a_{1g}$ orbital wave function of SF_6 and SCl_6. The continuous lines represent the values of the orbital with one sign; the dashed lines, the values with opposite sign. The contours near the atomic centers have been omitted: (a) SF_6; (b) SCl_6. (Note the different scale!)

II.[2] The orbital contour map of the SF_6 $2a_{1g}$ level shown in Figure 2a clearly confirms this view. This is, however, in strong contrast to the character of the corresponding $2a_{1g}$ level of SCl_6 (Figure 2b), which may be described as an antibonding sulfur 3s–chlorine 3s orbital. Is it possible to rationalize this finding by qualitative molecular orbital arguments? Three atomic orbitals or linear combinations thereof contribute to the molecular orbitals of symmetry a_{1g}: the sulfur 3s orbital and suitable linear combinations of ligand s and p orbitals. For the sake of argument, we switch on these interactions consecutively in Figure 3. In the first stage we observe a bonding and an antibonding linear combination of sulfur 3s and ligand s orbitals. By invoking this perturbational argument, it becomes clear that the interaction with the ligand p orbitals is stronger for fluorine than for chlorine so that the antibonding character of the $2a_{1g}$ level of SF_6 is overcome by the p_σ bonding contribution whereas in the chlorine case it is not. Therefore in contrast to the situation in SF_6, we find that the contributions of the $1a_{1g}$ and $2a_{1g}$ levels to sulfur–ligand bonding do not reinforce but partially cancel each other. This effect of the ligand s orbitals is not included in the usual discussion of the electronic structure of hypervalent molecules.[2] Our results show that it cannot always be neglected.

The orbital contour maps for the remaining occupied orbitals of SF_6 and SCl_6 are rather similar after proper scaling to account for the different bond lengths. If one measures the bond strength by overlap populations, as done in a LCAO-type formalism, the assumption of equal functional character for the overlap population density, differing only by a scaling of the coordinates, would imply a reduction by a factor of roughly $(d_{S-F}/d_{S-Cl})^3 \approx 0.5$ from SF_6 to SCl_6, again pointing to weaker bonds in SCl_6. The bonding of these molecules can satisfactorily be explained without invoking the stabilizing effect of sulfur d orbitals, a view which has been expressed many times.[2,8-11,12a] However, even the small influence of sulfur d orbitals decreases when going from SF_6 to SCl_6 (see the

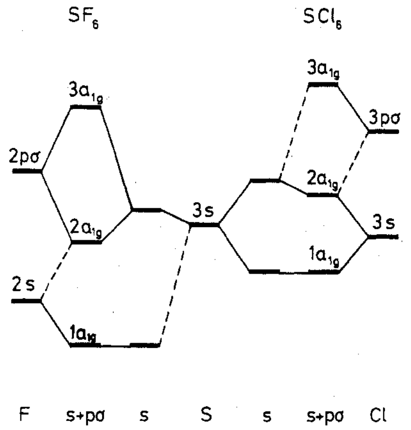

Figure 3. Interaction diagram for the σ-bonding orbitals in SF$_6$ (left) and SCl$_6$ (right). All other orbitals have been omitted. Weak interactions are indicated by dashed lines.

charge distribution in the sulfur sphere of the 1e$_g$, 1t$_{2g}$, and 2e$_g$ orbitals in Table I).

Our findings concerning the electronic structure of SH$_6$ qualitatively agree with those of earlier calculations.[2,10] The situation is similar to the one in SCl$_6$, in that the sulfur s contribution to bond formation is negligible. The fraction of charge of the 1a$_{1g}$ orbital localized in the sulfur sphere is 0.561, i.e., even larger than in the corresponding orbital of SCl$_6$.

To summarize, SCl$_6$ and SH$_6$ are expected to have much weaker bonds than SF$_6$. Also the steric situation around the sulfur atom is worse in SCl$_6$ than in SF$_6$. Unfortunately, we are not able to use total energies[17] in our argument on the existence of SCl$_6$ (for the discussion of the stability of SH$_6$, see ref 11). Since the bond strength is 58 kcal/mol in Cl$_2$ (vs. 37 kcal/mol in F$_2$), it appears improbable that the total energy of SCl$_6$ lies above that of SCl$_4$ + Cl$_2$.[18] In turn SCl$_4$ dissociates already at ~−30 °C into SCl$_2$ + Cl$_2$.[19]

Let us now examine the total charge distributions in the atomic, interatomic, and extramolecular regions of each molecule SX$_6$: Q_{S}, Q_{X}, Q_{INT}, and Q_{EXT}. These charges are listed in Table II together with $\Delta Q_i = Q_i^{\mathrm{mol}} - Q_i^{\mathrm{atom}}$ where Q_i^{mol} and Q_i^{atom} are the charge of a molecule in region i and the superimposed atomic charges in that region, respectively. From Table II we notice that every molecular electronic charge is contracted. Among the three, SH$_6$ undergoes the least change while the charge redistribution in SF$_6$ is quite significant. The net gain of electronic charge on the ligand side, defined by

$$\Delta = \sum_{i}^{\substack{\text{all}\\\text{ligands}}} \Delta Q_i - \Delta Q_{\mathrm{S}} \tag{7}$$

may be taken as a measure of the bond polarity. It describes how much more effective the ligands are in attracting the charge in regions II and III than is the central atom. This concept brings to mind a recently proposed formalism to determine the charge distribution in transition metal complexes via game theory.[20] Obviously, the Δ values of 0.653, 1.036, and 1.650 correlate with the electronegativity values of H, Cl, and F.[19] According to the above discussion on the stability of SCl$_6$ and SF$_6$, one might expect binding energies in the same ordering: SH$_6$ < SCl$_6$ < SF$_6$. The energies of the highest occupied molecular orbitals (HOMO) would also correlate with this relationship (see Figure 1). Therefore, the calculated Δ values imply that the Cl$_6$ lattice, not to mention the H$_6$ lattice, has less strength to withdraw the electronic charge from the sulfur atom than does the F$_6$ lattice. If charge removal of a sufficient amount is prerequisite for the formation of hypervalent molecules,[2a,6] the nonexistence of SH$_6$ and SCl$_6$ may be partially inferred from the resulting Δ values.[18]

Table II. Electronic Charges and Charge Differences (Molecular vs. Superposed Atomic Charges) in Different Molecular Regions for the SX$_6$ Series

Molecule	Q_{S}	Q_{X}	Q_{INT}	Q_{EXT}
SH$_6$	13.443	0.473	4.613	1.104
SCl$_6$	14.344	14.800	13.123	1.731
SF$_6$	13.671	7.023	12.303	1.886

Molecule	ΔQ_{S}	ΔQ_{X}	ΔQ_{INT}	ΔQ_{EXT}	Δ (ligand net gain)
SH$_6$	0.115	0.128	−0.226	−0.659	0.653
SCl$_6$	0.494	0.255	−0.735	−1.291	1.036
SF$_6$	0.702	0.392	−2.066	−0.994	1.650

As a final comment on the population analysis of these compounds it should be noted that neither the net charges of the sulfur atom (2.557, 1.656, and 2.329 for SH$_6$, SCl$_6$, and SF$_6$, respectively) nor the gross charges (1.898, −0.219, 0.571), as calculated according to eq 1 and 2 from the data in Table II, show any reasonable sizes or trends. This is a rather disappointing result which shows that the partitioning of space, necessary to establish the muffin tin approximation of the potential, bears a strong influence on any attributed atomic charges. Trends do show up, however, when considering differences ΔQ_i or "second" differences, such as Δ. It is also of value to compare the d-component populations ($\sum_m Q_{2m}{}^{\mathrm{S}}$ as defined in eq 5) in the sulfur sphere for the various SX$_6$-type molecules. The corresponding numbers are 0.344, 0.488, and 0.653 for SH$_6$, SCl$_6$, and SF$_6$, respectively. They correspond to 10, 11, and 18% of the total valence charge in the sulfur sphere of SH$_6$, SCl$_6$, and SF$_6$, respectively. These values show an interesting trend with the above inferred relative stability of the molecules, even if one takes the different sphere sizes into account. The value for SH$_6$ found from an LCAO–MO wave function[21] (0.244) lies below that found from the Xα–SW orbital wave function. When comparing this to Xα–SW populations, one should, however, keep in mind that the two values have been determined in rather different ways.

The Molecules SF$_4$ and SOF$_4$. The molecule sulfur tetrafluoride, SF$_4$, is the prototype of a type I hypervalent molecule.[2a] Its geometry may be idealized as a trigonal bipyramid with a sulfur lone pair in one of the equatorial positions (**1**).[22] The two equatorial S–F bonds are 2.920 au (F$_{\mathrm{eq}}$SF$_{\mathrm{eq}}$ = 101.5°), somewhat shorter than the S–F bond in SF$_6$ (2.956 au). The axial fluorine atoms are bonded to sulfur via hypervalent bonds which are significantly longer (3.111 au; F$_{\mathrm{ax}}$SF$_{\mathrm{ax}}$ = 187°). The two axial fluorines are bent somewhat to the side of the two equatorial ones. The molecule thionyl tetrafluoride SOF$_4$ (**2**) has roughly the same geometry with an oxygen occupying the third equatorial position. The

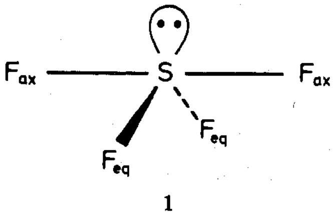

1

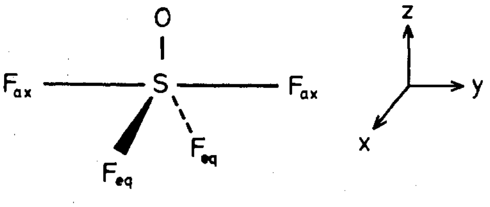

2

Table III. SCF–Xα–SW Orbital Energies and Normalized Charge Distributions in the Various Molecular Regions for the Valence Orbitals of SF_4

Orbital	$-\epsilon_i$[a]	S	F_{ax}	F_{eq}	INT	EXT
$1a_1$	2.638	0.119	0.052	0.262	0.245	0.007
$1b_1$	2.546	0.039	0.0	0.360	0.232	0.008
$1b_2$	2.435	0.033	0.393	0.0	0.165	0.016
$2a_1$	2.416	0.026	0.326	0.072	0.161	0.017
$3a_1$	1.723	0.455	0.068	0.093	0.205	0.018
$2b_1$	1.330	0.201	0.016	0.250	0.246	0.021
$2b_2$	1.288	0.193	0.199	0.075	0.234	0.026
$4a_1$	1.265	0.218	0.045	0.179	0.318	0.016
$1a_2$	1.152	0.015	0.091	0.241	0.304	0.017
$5a_1$	1.115	0.055	0.048	0.285	0.257	0.020
$3b_2$	1.101	0.039	0.189	0.147	0.268	0.026
$3b_1$	1.086	0.001	0.002	0.353	0.268	0.015
$4b_1$	1.007	0.003	0.344	0.032	0.224	0.021
$6a_1$	1.003	0.016	0.331	0.046	0.200	0.028
$4b_2$	0.993	0.008	0.257	0.122	0.224	0.011
$2a_2$	0.988	0.001	0.274	0.109	0.230	0.004
$6a_1$	0.897	0.210	0.263	0.016	0.204	0.029
$5b_1$	0.481	0.388	0.019	0.081	0.378	0.034
$8a_1$	0.300	0.262	0.045	0.094	0.336	0.125
$5b_2$	0.225	0.365	0.144	0.005	0.266	0.072

[a] Energies in rydbergs.

fluorine bond lengths and angles differ slightly from those in SF_4.[23] The geometry used was as follows:[23a] $d_{S-O} = 2.687$ au, $d_{S-F_{ax}} = 3.027$ au, $d_{S-F_{eq}} = 2.908$ au, $F_{eq}SF_{eq} = 123°$, $F_{ax}SF_{ax} = 183°$.

A number of molecular orbital calculations of SF_4[2c,24] or the related sulfurane SH_4[9,11,25] have appeared by now. A detailed molecular orbital analysis of bonding aspects, geometrical distortions, and substituent site preferences has been given recently.[9] Here, we are interested in a comparison of the electronic structures of SF_4, SOF_6, and SF_6 and in the difference between type I (SF_4) and type II (SOF_4, SF_6) hypervalent molecules.

Both molecules SF_4 and SOF_4 are of C_{2v} symmetry.[22,23] The irreducible representations of this group are labeled a_1, a_2, b_1, and b_2. With the exception of a_2 for which only two nonbonding orbitals occur, every irreducible representation has a basis in s and p type functions on all the centers. Therefore, even from symmetry arguments,[26] the question of d-orbital participation will not be relevant for these molecules. To improve the orbital wave functions and to be consistent with the calculation of SF_6 we included partial waves with $l = 2$ in the sulfur sphere. We come back to a quantitative discussion later on.

There is some ambiguity about how to choose the sphere radii in these low-symmetry molecules. The equatorial S–F bonds have approximately the same length as those in SF_6. We therefore require the continuity of the potential along these bonds. For touching spheres and centering the outer sphere on the sulfur atom, all other radii are then determined by geometry. The resulting atomic radii in SF_4 (and the corresponding values in SOF_4) are for sulfur 1.758 (1.753) au, for the equatorial fluorine atoms 1.162 (1.155) au, and for the axial fluorine atoms 1.353 (1.274) au. This leads to a rather small oxygen radius of 0.934 au leaving a large amount of the oxygen charge in the intersphere region. We thus decided to do an additional calculation with overlapping sulfur and oxygen spheres.[27] We enlarged the radius of the oxygen sphere in several calculations to a maximum of 1.20 au, a value which has been used for even shorter carbon–oxygen bonds.[28] None of the conclusions to be drawn depend critically on this parameter. We therefore present detailed results only for the calculation with overlapping spheres. The resulting energy levels are shown in Figure 4 together with those of the SF_6 molecule. Table III lists the charge distribution and energies for the occupied valence orbitals and the lower unoccupied orbitals of SF_4. In Table IV the same is done for the molecule SOF_4.

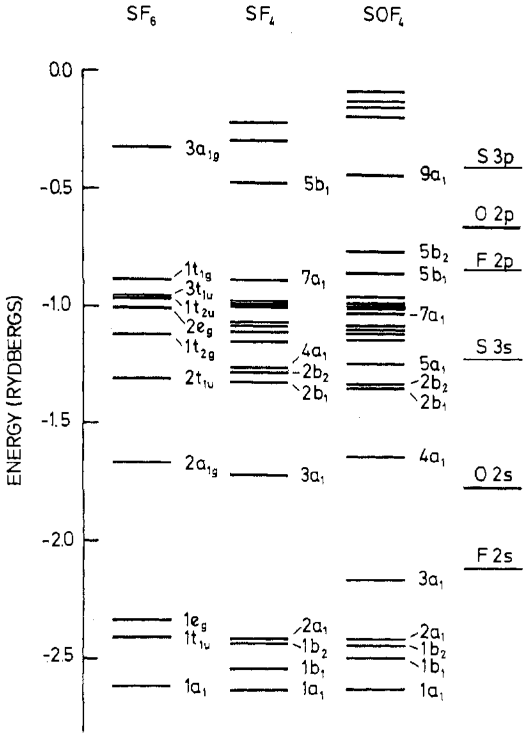

Figure 4. Comparison of the SCF-Xα-SW orbital energies for the molecules SF_6, SF_4, and SOF_4. For the sake of clarity only those levels are labeled which are discussed in the text. The highest occupied orbital is the $7a_1$ level in SF_4 and the $5b_2$ level in SOF_4.

Table IV. SCF–Xα–SW Orbital Energies and Normalized Charge Distributions in the Various Molecular Regions for the Valence Orbitals of the Molecule SOF_4 (Overlapping Sulfur and Oxygen Spheres)

Orbital	$-\epsilon_i$[a]	S	O	F_{ax}	F_{eq}	INT	EXT
$1a_1$	2.631	0.191	0.023	0.100	0.161	0.255	0.008
$1b_1$	2.499	0.053	0.0	0.0	0.344	0.246	0.012
$1b_2$	2.449	0.047	0.001	0.366	0.0	0.200	0.019
$2a_1$	2.421	0.038	0.017	0.205	0.157	0.204	0.017
$3a_1$	2.166	0.209	0.400	0.071	0.010	0.219	0.010
$4a_1$	1.647	0.315	0.125	0.052	0.104	0.225	0.024
$2b_1$	1.357	0.234	0.014	0.019	0.211	0.268	0.024
$2b_2$	1.332	0.234	0.017	0.206	0.033	0.234	0.035
$5a_1$	1.250	0.170	0.266	0.321	0.091	0.286	0.032
$1a_2$	1.146	0.024	0.0	0.125	0.182	0.335	0.026
$3b_2$	1.117	0.028	0.047	0.202	0.084	0.326	0.026
$6a_1$	1.104	0.046	0.043	0.023	0.274	0.296	0.023
$3b_1$	1.088	0.027	0.025	0.018	0.287	0.315	0.022
$7a_1$	1.035	0.075	0.098	0.230	0.066	0.197	0.038
$4b_1$	1.011	0.003	0.004	0.282	0.073	0.258	0.025
$4b_2$	1.006	0.009	0.003	0.141	0.210	0.271	0.015
$8a_1$	0.997	0.029	0.061	0.314	0.007	0.239	0.029
$2a_2$	0.968	0.000	0.0	0.222	0.152	0.229	0.023
$5b_1$	0.865	0.047	0.427	0.030	0.046	0.350	0.025
$5b_2$	0.772	0.011	0.487	0.075	0.0	0.332	0.019
$9a_1$	0.450	0.289	0.014	0.073	0.173	0.163	0.040
$6b_1$	0.201	0.388	0.137	0.012	0.095	0.231	0.031
$10a_1$	0.160	0.219	0.113	0.026	0.051	0.353	0.162
$11a_1$	0.133	0.031	0.021	0.005	0.011	0.398	0.518
$6b_2$	0.092	0.420	0.019	0.153	0.017	0.153	0.067

[a] Energies in rydbergs.

In the following molecular orbital analysis we shall make use of these data, orbital contour maps and a partial wave population analysis (see above) from which the general shape

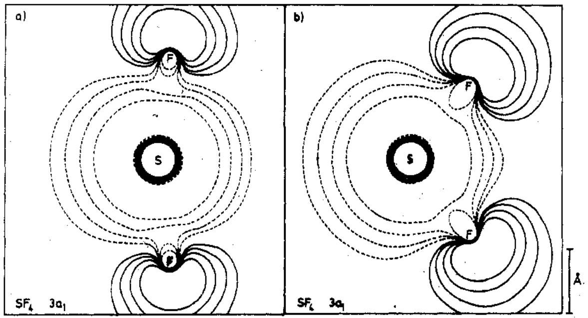

Figure 5. Contour plots of the $3a_1$ orbital in SF_4 showing the interaction of the sulfur 3s atomic orbital and the ligand orbitals. The set of contour values is the same as those in Figure 2: (a) plane defined by the axial ligands, $F_{ax}SF_{ax}$; (b) plane defined by the equatorial ligands, $F_{eq}SF_{eq}$.

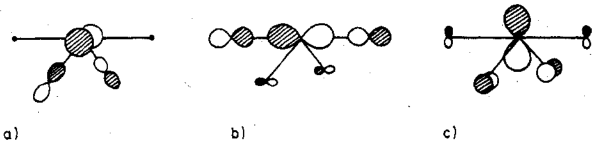

Figure 6. Schematic representation of those orbitals of SF_4 which show the sulfur 3p contribution to bonding: (a) the $2b_2$ orbital; (b) the $2b_1$ orbital; (c) the $4a_1$ orbital.

of the orbitals may be inferred as well.

At first sight, one discovers from Figure 4 a large similarity between the energy level schemes of all three molecules SF_6, SF_4, and SOF_4. The levels $1a_1$, $1b_1$, $1b_2$, and $2a_1$ are mainly derived from fluorine 2s orbitals as may be seen from their energies and the population analysis. The first three of them contribute to sulfur–fluorine bonding, the $1a_1$ level with a strong 3s character in the sulfur sphere very much so, whereas the $2a_1$ orbital is largely a nonbonding in-phase combination of the two axial F 2s orbitals. These findings parallel the situation found in SF_6 (see above). This is true also for the $3a_1$ level (cf. $2a_{1g}$ in SF_6) whose localization in the sulfur sphere has increased to 0.455 in agreement with the expectation for type I hypervalent bonding. But, nevertheless, it contributes to sulfur–fluorine bonding much in the same way as does the corresponding $2a_{1g}$ level in SF_6. This may be seen by comparing the contour map of this orbital (see Figure 2a) to the two contour maps in Figure 5 which show the $3a_1$ orbital in the planes defined by $F_{ax}SF_{ax}$ and $F_{eq}SF_{eq}$. The next three levels, $2b_1$, $2b_2$, and $4a_1$, may formally be derived from the $2t_{1u}$ level in SF_6 when going from O_h symmetry to C_{2v} in SF_4. Their shapes are sketched out in Figure 6 to show how the 3p orbitals of sulfur participate in the bonding with the fluorine 2p orbitals. Some small contributions of π bonding are found in the orbitals $2b_1$ and $4a_1$. The next eight orbitals on the energy scale ($1a_2$–$2a_2$) are nonbonding and delocalized over the ligands.

The HOMO ($7a_1$) lies somewhat separated in energy. There has been some controversy whether it should contain mainly the sulfur lone pair[9] or should be delocalized over the axial ligands[2c,11] containing the extra electrons of the electron-rich hypervalent bond. In our calculation we find it to be a combination of both (see Figure 7a), thus partially confirming the prediction made by Chen and Hoffmann.[9] Of course, the sulfur lone pair will be smeared out over several levels in a molecular orbital approach. However, we find an appreciable localization of p_z character only in the $4a_1$ (0.192) and $7a_1$ orbitals (0.116).

Comparing the axial and the equatorial sulfur–fluorine bonds one notices that the orbitals describing the axial bonds ($1b_2$, $2b_2$) lie energetically higher than the corresponding ones for the equatorial bonds ($1b_1$, $2b_1$). In addition, there is the $4a_1$ orbital which reinforces the latter bonds. Both observations are consistent with the equatorial bonds being stronger than the axial ones.

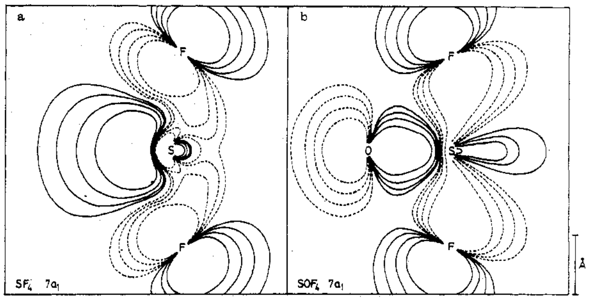

Figure 7. Contour plots of the HOMO $7a_1$ in SF_4 and the orbital $7a_1$ in SOF_4 derived from it. The planes shown are the same in both cases, defined by the axial fluorine atoms and the third equatorial position which is empty in SF_4 and occupied by oxygen in SOF_4: (a) SF_4; (b) SOF_4.

The results of our molecular orbital calculation of SF_4 support the conclusions from simple MO theoretical arguments[9] concerning the energy level scheme and the general aspects of bonding. They do not justify the distinction made by the theory of hypervalent molecules[2a,c] into different hybridization schemes since the relative contribution of the sulfur 3s orbital to the ligand bonding varies only slightly in going from SF_6 to SF_4. The agreement with the calculations by Koutecky and Musher[2c] using the CNDO/2 method is very qualitative.[29] They found the bonding levels in the order $4a_1 < 2b_1 < 2b_2$, a much stronger S–F π bond (judging qualitatively from their figures), and a HOMO without any sulfur lone-pair contribution. Since the method employed is quite different from ours, the above differences are not unexpected. The agreement between the present work and other simplified treatments[24] is also rather qualitative.

The level structure of SOF_4 differs from that of SF_4 mainly through the (additional) levels $3a_1$, $5b_1$, and $5b_2$. The extreme localization of the $5b_1$ and $5b_2$ levels clearly discriminates these highest lying occupied molecular orbitals as describing oxygen lone pairs. The $7a_1$ HOMO of SF_4 underwent a remarkable stabilization in SF_4O ($\Delta\epsilon_i = -0.138$ Ry) where the $7a_1$ orbital shows most of its former character (see Figure 7b). The strong oxygen–sulfur bond is usually taken as a double bond.[30] The levels $3a_1$ (mainly O 2s–S 3s), $5a_1$ (mainly O 2p–S 3p), and $7a_1$ show bonding character between oxygen and sulfur whereas the $4a_1$ orbital is oxygen–sulfur antibonding. The contribution of the fluorine ligands to various other levels in SOF_4 remains more or less unchanged from that in SF_4.

Photoelectron measurements have been reported only for the fluorine 1s levels in SF_4.[31] We do find the axial fluorine atoms to have smaller ionization energies (678.5 vs. 683.9 eV) from transition-state calculations[16] in agreement with the expected larger negative charge on the axial fluorine atoms. However, the quantitative agreement with experiment (692.9 vs. 695.3 eV) is rather poor. It might possibly be improved by localizing the "hole" on a definite ligand atom.[32] No experimental valence-shell photoelectron spectra are available for either SF_4 or SOF_4. We therefore carried out transition-state calculations[16] only for the orbitals of a_1 symmetry. The relaxation downward in energy is rather uniform and amounts to approximately 4 eV. This leads to first ionization potentials of 16.2 and 14.5 eV for SF_4 and SOF_4, respectively. The general structure of the spectra should parallel that of the corresponding one-electron energies as shown in Figure 4.

Let us now turn to the charge distribution and population analysis of these compounds. The relevant data are collected in Table V. Again we notice that charge contraction occurs

Table V. Electronic Charges and Charge Differences in Different Molecular Regions of SF_4, SOF_4, and SF_6

Molecule	Q_S	$Q_{F_{ax}}$	$Q_{F_{eq}}$	Q_O	Q_{INT}	Q_{EXT}
SF_4	13.276	7.796	7.286		7.969	0.590
SOF_4	13.554	7.291	6.845	4.985	12.782	0.396
SOF_4[a]	13.581	7.429	6.985	6.118	10.568	0.903
SF_6[b]	13.671		7.023		12.303	1.886

Molecule	ΔQ_S	$\Delta Q_{F_{ax}}$	$\Delta Q_{F_{eq}}$	ΔQ_O	ΔQ_{INT}	ΔQ_{EXT}	Δ (ligand net gain)
SF_4	0.406	0.526	0.706		−2.201	−0.650	2.058
SOF_4	0.674	0.311	0.335	0.645	−1.248	−1.372	1.263
SOF_4[a]	0.701	0.449	0.475	0.515	−2.181	−0.865	1.662
SF_6[b]	0.702		0.392		−2.066	−0.994	1.660

[a] Overlapping-sphere parameterization. [b] All fluorine atoms are equivalent, of course.

in each atomic region of these molecules (cf. Table II and part 1) and that the ligands accumulate more than does the central sulfur atom (net gain $\Delta > 0$). The axial fluorine atoms in SF_4 have a larger amount of charge associated with them than the equatorial ligands. The analysis of photoelectron spectra[31] and the population analysis of LCAO–MO wave function[2c,24] show the same trend. It is interesting to note that the charge increase in the equatorial fluorine spheres is larger although their size is smaller. In other words, more electronic charge contraction occurs around the equatorial bond regions. Following the findings in part 1, the equatorial S–F bonds are predicted to be stronger than the axial bonds, which is in agreement with our analysis of the individual MO's, other calculations,[9,24d] and experiment.[22,30,33]

In the case of SOF_4, the charge distribution on the fluorine atoms of the two different environments shows the same trends as found in SF_4. The fact that the charge increase in the oxygen sphere is larger than that in the fluorine spheres may be considered as due to the double-bond character of the sulfur–oxygen bond. In the overlapping sphere parametrization these differences tend to be equalized.

The ligand net gain Δ in SF_4 is quite large whereas Δ values for SOF_4 and SF_6 are rather comparable. The same relation is observed in the Xα–SW gross charges on sulfur: 1.130 in SF_4, 0.657 in SOF_4, and 0.571 in SF_6. The gross charges on the fluorine atoms in SF_4 are −0.537 (axial) and −0.028 (equatorial). The ligand charge in SF_6 (−0.095) lies between them as was found in other calculations.[24d-f,31] The difference between axial and equatorial ligand charges is, however, rather large and partly due to the different sphere sizes. It has been concluded from LCAO calculations[11,24] that the sulfur charge increases with the number of ligands. Neither Xα–SW net nor gross charges show this trend as a comparison of the results for SF_4 and SF_6 reveals, although the sulfur sphere sizes of these molecules are quite comparable (1.758 vs. 1.780 au). One might be tempted to speculate whether the fact that the electronic charge of the sulfur atom is more easily drained in SX_4 than in SX_6 by the electronegative atoms X may be one reason why SCl_6 does not exist but SCl_4 does.

A detailed analysis of the Xα–SW orbital wave functions shows that the fractions of s (28%) and p (72%) valence electron populations in the fluorine atoms stay remarkably constant regardless of the ligand type (axial vs. equatorial) and the molecule (SF_4, SOF_4, and SF_6). The corresponding analysis of the sulfur valence electrons is given in Table VI. Again, SOF_4 and SF_6 look rather similar, where the s population in SF_4 has been increased at the expense of the d orbital contribution. This effect is almost exclusively a consequence of the strong localization of the "sulfur 3s" orbital $3a_1$ in SF_4. It may be interpreted as a somewhat smaller mixing of the sulfur 3s with the ligand orbitals in this compound. This difference may therefore be ultimately traced back to Musher's distinction between type I (SF_4) and type II (SOF_4, SF_6) bonding. However, two such separate theoretical concepts only obscure the large similarities in the electronic structure of these molecules as our discussion has brought out.

Table VI. Population Analysis (Absolute and Relative) of the Valence Electrons Located in the Sulfur Sphere for SF_4, SOF_4, and SF_6

Molecule	s	p	d	Total
SF_4	1.320 (40%)	1.658 (51%)	0.298 (9%)	3.276
SOF_4[a]	1.148 (32%)	1.852 (52%)	0.581 (16%)	3.581
SF_6	1.148 (31%)	1.870 (51%)	0.653 (18%)	3.671

[a] Overlapping-sphere parameterization.

Acknowledgment. This research was supported in part by the National Research Council of Canada and by the Deutsche Forschungsgemeinschaft. We wish to thank Professor K. H. Johnson for his kindness in furnishing the original version of the computer programs used in this study and Professor K. Weiss for helpful comments about a preliminary version of this paper. This work was completed at the Technical University of Munich during a stay of V.H.S., who gratefully acknowledges the kind hospitality extended to him by Professor G. L. Hofacker.

Registry No. SH_6, 51715-67-4; SCl_6, 38158-58-6; SF_6, 2551-62-4; SF_4, 7783-60-0; SOF_4, 13709-54-1.

References and Notes

(1) (a) Technische Universität München. (b) Queen's University.
(2) (a) J. I. Musher, *Angew. Chem.*, **81**, 68 (1969); (b) J. I. Musher, *J. Am. Chem. Soc.*, **94**, 1370 (1972); (c) V. B. Koutecky and J. I. Musher, *Theor. Chim. Acta*, **33**, 227 (1974); (d) H. Nakatsuji and J. I. Musher, *Chem. Phys. Lett.*, **24**, 77 (1974).
(3) K. A. Mitchell, *Chem. Rev.*, **69**, 157 (1969).
(4) L. Pauling, "The Nature of the Chemical Bond", 3d ed, Cornell University Press, Ithaca, N.Y., 1960.
(5) G. Dogett, *Theor. Chim. Acta*, **15**, 344 (1969).
(6) C. A. Coulson, *Nature (London)*, **221**, 1106 (1969).
(7) C. A. Coulson and F. A. Gianturco, *J. Chem. Soc. A*, 1618 (1968).
(8) R. E. Rundle, *Surv. Prog. Chem.*, **1**, 81 (1963).
(9) M. M. L. Chen and R. Hoffmann, *J. Am. Chem. Soc.*, **98**, 1647 (1976).
(10) N. Rösch, V. H. Smith, Jr., and M. H. Whangbo, *J. Am. Chem. Soc.*, **96**, 5984 (1974).
(11) G. M. Schwenzer and H. F. Schaefer, III, *J. Am. Chem. Soc.*, **97**, 1393 (1975).
(12) (a) K. H. Johnson, *Annu. Rev. Phys. Chem.*, in press; (b) J. C. Slater and K. H. Johnson, *Phys. Rev. B*, **5**, 844 (1972); (c) K. H. Johnson and F. C. Smith, Jr., *ibid.*, **5**, 831 (1972); (d) K. H. Johnson, *Adv. Quantum Chem.*, **7**, 143 (1973).
(13) Cf. N. Rösch and D. Menzel, work to be submitted for publication, where the atomic orbital populations $Q_{lm}^{(i)}$ defined herein (eq 5) have been successfully applied to the problem of s–d mixing in transition metal clusters.
(14) See also J. W. D. Connolly and K. H. Johnson, *Chem. Phys. Lett.*, **10**, 616 (1971), where a slightly different bond length was used.
(15) (a) K. Schwarz, *Phys. Rev. B*, **5**, 2466 (1972); (b) S. R. Singh and V. H. Smith, Jr., *Phys. Rev. A*, **4**, 1774 (1971).
(16) J. C. Slater, *Adv. Quantum Chem.*, **6**, 1 (1972).
(17) For a discussion of the accuracy of Xα–SW total energies derived from muffin tin charge densities see, e.g., (a) J. W. D. Connolly and J. R. Sabin, *J. Chem. Phys.*, **56**, 5529 (1972); (b) J. B. Danese and J. W. D. Connolly, *ibid.*, **61**, 3063 (1974); (c) U. Mitzdorf, *Theor. Chim. Acta*, **37**, 129 (1975).
(18) W. E. Dasent, "Nonexisting Compounds", Marcel Dekker, New York, N.Y., 1965, p 153.
(19) F. A. Cotton and G. Wilkinson, "Advanced Inorganic Chemistry", 3d ed, Interscience, New York, N.Y., 1972.
(20) W. Haberditzl and H.-G. Bartel, *Chem. Phys. Lett.*, **19**, 432 (1973).
(21) When six d-like functions (x^2, xy, y^2, yz, z^2, and xz) are included in an LCAO basis, one has to keep in mind that one proper linear combination actually is s-like. In a straightforward Mulliken population analysis one will therefore find a spurious d-orbital contribution which properly should be added to the s population. See for instance a "d-orbital" population of −0.131 in the $3a_{1g}$ level of SH_6 as found in Table IV of ref 11. The proper value for the total d population is therefore exclusively given by the $1e_g$ orbital: 0.244. Such a correction should, of course, also be made

to the populations of SH_2 and SH_4 given in that table but cannot be done with the given data on symmetry arguments alone.

(22) W. M. Tolles and W. D. Gwinn, *J. Chem. Phys.*, **36**, 1119 (1962).

(23) (a) J. L. Hencher, D. W. J. Cruickshank, and S. H. Bauer, *J. Chem. Phys.*, **48**, 518 (1968); (b) G. Gundersen and K. Hedberg, *ibid.*, **51**, 2500 (1969).

(24) (a) R. D. Willett, *Theor. Chim. Acta*, **2**, 393 (1964); (b) D. P. Santry and G. A. Segal, *J. Chem. Phys.*, **47**, 158 (1967); (c) D. P. Santry, *J. Am. Chem. Soc.*, **90**, 3309 (1968); (d) R. D. Brown and J. B. Peel, *Aust. J. Chem.*, **21**, 2589, 2605 (1968); (e) A. Breeze, D. W. J. Cruickshank, and D. R. Armstrong, *J. Chem. Soc., Faraday Trans. 2*, **68**, 2144 (1972); (f) R. G. Hyde, J. B. Peel, and K. Terauds, *J. Chem. Soc., ibid.*, **69**, 1563 (1973).

(25) R. Gleiter and A. Veillard, *Chem. Phys. Lett.*, **37**, 33 (1976).

(26) M. A. Ratner and J. R. Sabin, *J. Am. Chem. Soc.*, **93**, 3542 (1971).

(27) (a) N. Rösch, W. G. Klemperer, and K. H. Johnson, *Chem. Phys. Lett.*, **23**, 149 (1973); (b) F. Herman, A. R. Williams, and K. H. Johnson, *J. Chem. Phys.*, **61**, 3506 (1974).

(28) I. P. Batra and O. Robaux, *Chem. Phys. Lett.*, **28**, 529 (1974).

(29) Apparently there are quite a few wrong symmetry assignments in Figure 4 and Table I of ref 2c which makes the comparison of our results with those of ref 2c somewhat uncertain.

(30) H. H. Szmant in "Sulfur in Organic and Inorganic Chemistry", Vol. 1, A. Senning, Ed., Marcel Dekker, New York, N.Y., 1971, p 107.

(31) R. W. Shaw, Jr., T. X. Carroll, and T. D. Thomas, *J. Am. Chem. Soc.*, **95**, 5870 (1973).

(32) J. W. D. Connolly, U. Gelius, C. Nordling, and H. Siegbahn, *J. Chem. Phys.*, **58**, 4265 (1973).

(33) (a) W. C. Smith, *Angew. Chem., Int. Ed. Engl.*, **1**, 467 (1962); (b) S. M. Williamson, *Prog. Inorg. Chem.*, **7**, 39 (1966).

Contribution from the Chemistry Department,
University of Southern California, Los Angeles, California 90007

Microwave Spectrum, Structure, and Dipole Moment of 1,7-Dicarba-*closo*-octaborane(8), $C_2B_6H_8$

HARVEY N. ROGERS, KAR-KUEN LAU, and ROBERT A. BEAUDET*

Received December 3, 1975 AIC50870J

The microwave spectrum of 1,7-dicarba-*closo*-octaborane(8), $C_2B_6H_8$, has been observed and the rotational spectra of nine isotopic species have been assigned. Coordinates of all boron atoms were accurately located and boron–boron bond lengths were determined. The results support those of earlier x-ray diffraction studies and confirm that the slightly distorted D_{2d} geometry of the C_2B_6 unit exists in the gas phase. The bond distances are B_2–B_3 = 1.813 Å, B_2–B_5 = 1.843 Å, B_2–B_6 = 1.685 Å, B_3–B_4 = 1.886 Å, B_3–B_6 = 1.880 Å, and B_5–B_6 = 1.949 Å. The molecular dipole was measured to be μ = 1.40 + 0.01 D.

Introduction

The structure of the carborane 1,7-$C_2B_6H_8$ has been the topic of much discussion. Williams and Gerhart proposed a dodecahedral structure similar to that of B_8Cl_8[1] based on the mass spectrum and ^{11}B NMR data.[2] More recently, proton NMR and ^{11}B NMR analyses of the *C,C′*-dimethyl derivative have indicated the equivalence of the methyl groups and their adjacent carbon atoms.[3] These data are consistent with a square-antiprismatic structure. Single-crystal x-ray diffraction studies have shown the structure to consist of a dodecahedron which is distorted toward a square antiprism.[4] These results indicate a molecule with C_2 symmetry which exhibits chirality. To confirm that this molecule retains its distorted chiral structure in the gas phase the microwave spectrum was investigated and the structure of the boron atoms was determined. The dipole moment was also obtained.

Experimental Section

Previously, the carborane 1,7-$C_2B_6H_8$ had been prepared by the pyrolysis of 1,3-dicarbanidononaborane(13), $C_2B_7H_{13}$, in diphenyl ether. By using an improved synthesis described by Dunks and Hawthorne,[5] the yield of 1,7-$C_2B_6H_8$ has been doubled. A 60% yield is obtained by slow, low-pressure pyrolysis of $C_2B_7H_{13}$. The original sample of $C_2B_6H_8$ was kindly provided by T. Onak. The sample was stored in a Pyrex tube in liquid nitrogen without further purification. No problems involving impurity or decomposition were encountered. The microwave spectrum between 8 and 40 GHz was observed at dry ice temperature and at pressures between 10 and 50 mTorr. A standard 100-kHz Stark-modulated spectrometer was used in this investigation. Frequency measurements were calibrated by using a General Radio Co. standard frequency multiplier, Type 1112-A, with a Hewlett-Packard HP5245L electronic counter. Stark effects were studied by D.C. biasing the 100-kHz square wave. The effective waveguide spacing was determined by measuring the Stark shifts of the $J = 1 \leftarrow 0$ transitions of carbonyl sulfide.

Table I. Rotational Constants[a] of the Isotopic Species of 1,7-$C_2B_6H_8$

Isotopic species	Rel intens[b]	*A*, MHz	*B*, MHz	*C*, MHz
Normal	1	3885.03	3124.79	3091.11
2-^{10}B	0.47	3902.60	3168.02	3129.77
3-^{10}B	0.47	3932.73	3148.87	3102.46
5-^{10}B	0.47	3936.42	3148.20	3102.41
2,4-^{10}B	0.11	3950.88	3195.05	3137.75
2,5-^{10}B	0.11	3954.51	3187.74	3145.86
2,6-^{10}B	0.11	3954.40	3195.58	3138.62
3,5-^{10}B	0.11	3984.03	3178.81	3107.45
3,6-^{10}B	0.11	3985.41	3159.25	3126.70

[a] Uncertainties are 0.04 MHz or less. [b] The natural abundance ratio of ^{10}B:^{11}B is 19:81.

Spectra

Initial predictions of the rotational constants were made using the skeletal structural parameters of 1,7-$B_6H_8C_2(CH_3)_2$.[4] Such predictions indicated that $C_2B_6H_8$ is a near-prolate symmetric rotor with the principal axes directed as shown in Figure 1. The point symmetry of the molecule is C_2; the C_2 axis is coincident with the inertial *c* axis and passes through the midpoints of the B(3)–B(4) bond and the B(5)–B(6) bond. The dipole moment of the parent species lies only along the *c*-axis direction, however small *a* and *b* dipole components are present in certain species when the axes are rotated upon isotopic substitution. Nevertheless, only *c*-type transitions were observable for all boron isotopic species.

Most of the boron isotopic species exist in sufficient concentrations to be observed in natural abundance. Assignment of a value of 1 to the intensity of the normal species gives relative intensities of various substituted boron isotopes as listed in Table I. Most species were assigned on the basis of Stark effects and relative intensities. The relative intensity pattern for the isotopic species is consistent with the relative abundance of the isotopes of a molecule belonging to a C_2 point group. In principle, the variation in intensities due to nuclear spin statistics can also be used; however calculations reveal the differences are too small to be useful. Four doubly substituted species and the ^{13}C species were too weak to be observed.